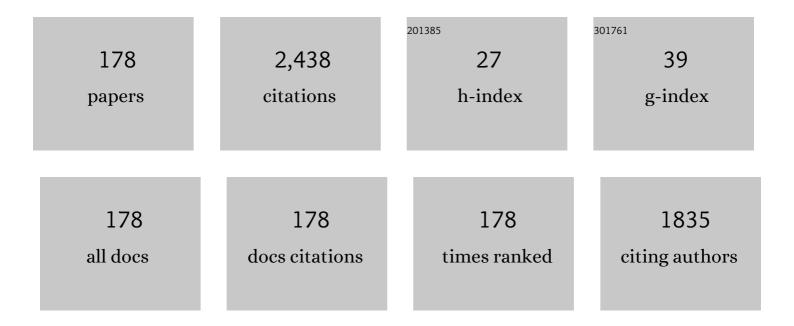
Han-Choel Choe

List of Publications by Year in descending order

Source: https://exaly.com/author-pdf/8122593/publications.pdf Version: 2024-02-01



#	Article	IF	CITATIONS
1	Precipitation of bone-like apatite on plasma electrolytic oxidized Ti-6Al-4V alloy. Thin Solid Films, 2022, 746, 139136.	0.8	7
2	Electrochemical characteristics of Sr/Si-doped hydroxyapatite coating on the Ti alloy surface via plasma electrolytic oxidation. Thin Solid Films, 2022, 746, 139124.	0.8	8
3	A new link between apoptosis induced by the metformin derivative HL156A and autophagy in oral squamous cell carcinoma. European Journal of Pharmacology, 2022, 920, 174859.	1.7	3
4	Micro-scaled morphology of Ti-40Nb-xZr alloy with applied voltage via plasma electrolytic oxidation. Thin Solid Films, 2022, 751, 139231.	0.8	3
5	Nanotube Formation of Ti-6Al-4V Alloy and Its Corrosion Behavior. Thin Solid Films, 2022, , 139216.	0.8	2
6	Surface Characteristics of Dental Implant Doped with Si, Mg, Ca, and P Ions via Plasma Electrolytic Oxidation. Journal of Korean Institute of Metals and Materials, 2022, 60, 263-271.	0.4	2
7	Corrosion behaviors of macro/micro/nano-scale surface modification on Ti-6Al-4V alloy for bio-implant. Thin Solid Films, 2022, 754, 139314.	0.8	7
8	Surface characteristics of plasma electrolytic oxidized Ti-mesh for dental use. Korean Journal of Dental Materials, 2022, 49, 63-76.	0.2	0
9	Nanotube shape changes on Ti-6Al-4ÂV alloy via various applied potential for bio-implants. Applied Nanoscience (Switzerland), 2022, 12, 3329-3336.	1.6	1
10	Simultaneous improvement of corrosion resistance and bioactivity of a titanium alloy via wet and dry plasma treatments. Journal of Alloys and Compounds, 2021, 851, 156840.	2.8	47
11	Bioactive element coatings on nano-mesh formed Ti-6Al-4V alloy surface using plasma electrolytic oxidation. Surface and Coatings Technology, 2021, 406, 126649.	2.2	13
12	Acceleration of Bone Formation and Adhesion Ability on Dental Implant Surface via Plasma Electrolytic Oxidation in a Solution Containing Bone Ions. Metals, 2021, 11, 106.	1.0	20
13	Nano/Micro-Sized Morphologies of Hydroxyapatite Coatings Containing Mn and Si on an Oxidized Ti–6Al–4V Alloy Surface for Dental Implants. Journal of Nanoscience and Nanotechnology, 2021, 21, 3701-3706.	0.9	2
14	Plasma Electrolytic Oxidation on Ti–xNb–2Ag–2Pt Alloys for Nano- and Micro-Pore Formation in Electrolyte with Ca and P Ions for Dental Implant Use. Journal of Nanoscience and Nanotechnology, 2021, 21, 3753-3758.	0.9	1
15	Electrochemical Analysis of Nano- and Micro-Sized Pore Formed Ti–6Al–4V Alloys in Solution Containing Ca, P, Mn, and Si Ions via Plasma Eletrolytic Oxidation for Bio-Implant Materials. Journal of Nanoscience and Nanotechnology, 2021, 21, 4022-4028.	0.9	2
16	Nanotube Morphology Changes of Ti– <i>x</i> Ta–Ag–Pt Alloys with Ta Content for Biomaterials. Journal of Nanoscience and Nanotechnology, 2021, 21, 4807-4812.	0.9	0
17	Morphology of hydroxyapatite and Sr coatings deposited using radio frequency-magnetron sputtering method on nanotube formed Ti-6Al-4V alloy. Thin Solid Films, 2021, 735, 138893.	0.8	6
18	The effect of in-situ reactive incorporation of MoOx on the corrosion behavior of Ti-6Al-4ÂV alloy coated via micro-arc oxidation coating. Corrosion Science, 2021, 192, 109764.	3.0	32

#	Article	IF	CITATIONS
19	Surface characteristics of nanotube-formed Ti-Ta-Ag-Pt alloys for dental implants. Korean Journal of Dental Materials, 2021, 48, 191-210.	0.2	0
20	Plasma electrolytic oxidized surface of (Mg/Si)-hydroxyapatite coated Ti-29Nb-xHf alloys for dental implant. Korean Journal of Dental Materials, 2021, 48, 255-268.	0.2	1
21	Triggering the hydroxyapatite deposition on the surface of PEO-coated Ti–6Al–4V alloy via the dual incorporation of Zn and Mg ions. Journal of Alloys and Compounds, 2020, 819, 153038.	2.8	59
22	Highly Ordered Nanotube Formation on Beta Typed Ti–xTa Alloy Surface. Journal of Nanoscience and Nanotechnology, 2020, 20, 5791-5795.	0.9	1
23	Magnesium, silicon, and hydroxyapatite deposition on the Ti-xNb-2Ag-2Pt alloy by co-sputtering after nanotube formation. Surface and Coatings Technology, 2020, 404, 126487.	2.2	9
24	Plasma electrolytic oxidation of Ti-6Al-4V alloy in electrolytes containing bone formation ions. Applied Surface Science, 2020, 513, 145776.	3.1	17
25	Functional element coatings on Ti-alloys for biomaterials by plasma electrolytic oxidation. Thin Solid Films, 2020, 699, 137896.	0.8	11
26	Plasma electrolytic oxidation of Ti-25Nb-xTa alloys in solution containing Ca and P ions. Surface and Coatings Technology, 2020, 395, 125916.	2.2	32
27	Corrosion Behaviors of Zn, Si, and Mn-Doped Hydroxyapatite Coatings Formed on the Ti–6Al–4V Alloy by Plasma Electrolytic Oxidation. Journal of Nanoscience and Nanotechnology, 2020, 20, 5618-5624.	0.9	2
28	Nanotube Morphology Changes on the Ti–xNb–Ag–Pt Alloy with Nb Contents. Journal of Nanoscience and Nanotechnology, 2020, 20, 5751-5754.	0.9	1
29	Surface Observation of Plasma Electrolytic Oxidation-Treated Ti–6Al–4V Alloy After 2-Step Nano-Mesh Formation. Journal of Nanoscience and Nanotechnology, 2020, 20, 5755-5758.	0.9	Ο
30	Corrosion behaviors of bioactive element coatings on PEO-treated Ti-6Al-4V alloys. Surface and Coatings Technology, 2019, 376, 44-51.	2.2	23
31	Functional Elements Coatings on Ti–6Al–4V Alloy by Plasma Electrolytic Oxidation for Biomaterials. Journal of Nanoscience and Nanotechnology, 2019, 19, 1114-1117.	0.9	2
32	Electrochemical and bioactive characteristics of the porous surface formed on Ti-xNb alloys via plasma electrolytic oxidation. Surface and Coatings Technology, 2019, 378, 125027.	2.2	46
33	Surface morphology and cell behavior of Zn-coated Ti-6Al-4V alloy by RF-sputtering after PEO-treatment. Surface and Coatings Technology, 2019, 361, 386-395.	2.2	19
34	Bioactive apatite formation on PEO-treated Ti-6Al-4V alloy after 3rd anodic titanium oxidation. Applied Surface Science, 2019, 484, 365-373.	3.1	29
35	Functional Elements Coatings on the Plasma Electrolytic Oxidation-Treated Ti–6Al–4V Alloy by Electrochemical Precipitation Method. Journal of Nanoscience and Nanotechnology, 2019, 19, 4344-4349.	0.9	11
36	Surface observation of nanotube-formed titanium by anodization in electrolyte containing hydroxyapatite nanoparticles. Applied Surface Science, 2019, 483, 76-84.	3.1	10

#	Article	IF	CITATIONS
37	Evaluation of bone formation on ultra-fine structures in simulated body fluid. Applied Surface Science, 2019, 477, 271-279.	3.1	10
38	Morphology changes and bone formation on PEO-treated Ti-6Al-4V alloy in electrolyte containing Ca, P, Sr, and Si ions. Applied Surface Science, 2019, 477, 121-130.	3.1	27
39	Corrosion phenomena of PEO-treated films formed in solution containing Mn, Mg, and Si ions. Applied Surface Science, 2019, 477, 50-59.	3.1	21
40	Effects of Zn and Si ions on the corrosion behaviors of PEO-treated Ti-6Al-4V alloy. Applied Surface Science, 2019, 477, 79-90.	3.1	20
41	Hydroxyapatite coatings containing Zn and Si on Ti-6Al-4Valloy by plasma electrolytic oxidation. Applied Surface Science, 2018, 432, 337-346.	3.1	28
42	Mg-containing hydroxyapatite coatings on Ti-6Al-4V alloy for dental materials. Applied Surface Science, 2018, 432, 294-299.	3.1	17
43	Ultra-fine structures of Pd-Ag-HAp nanoparticle deposition on protruded TiO 2 barrier layer for dental implant. Applied Surface Science, 2018, 432, 285-293.	3.1	9
44	Mn-coatings on the micro-pore formed Ti-29Nb-xHf alloys by RF-magnetron sputtering for dental applications. Applied Surface Science, 2018, 432, 278-284.	3.1	20
45	A Simulated Body Fluid Evaluation of TiO2 Barrier Oxide Layer Formed by Electrochemical Reaction. Journal of Nanoscience and Nanotechnology, 2018, 18, 2058-2062.	0.9	1
46	Electrochemical Deposition of Hydroxyapatite Substituted with Magnesium and Strontium on Ti–6Al–4V Alloy. Journal of Nanoscience and Nanotechnology, 2018, 18, 1449-1452.	0.9	6
47	Pore Shape Changes and Apatite Formation on Zn and Si Ion-Doped HA Films of Ti-6Al-4V After Plasma Electrolytic Oxidation Treatment. Journal of Nanoscience and Nanotechnology, 2018, 18, 1442-1444.	0.9	3
48	Hydroxyapatite Coatings Containing Mn and Si on the Oxidized Ti-6Al-4V Alloy for Dental Applications. Journal of Nanoscience and Nanotechnology, 2018, 18, 833-836.	0.9	5
49	Morphology Changes of Plasma Electrolytic Oxidized Ti–6Al–4V Alloy in the Electrolytes Containing Sr and Si Ions. Journal of Nanoscience and Nanotechnology, 2018, 18, 1453-1456.	0.9	0
50	Effects of Hf content on nanotubular structure of Ti-29Nb-xHf ternary alloys. Surface and Coatings Technology, 2017, 320, 109-117.	2.2	6
51	Biocompatibility and Degradation of a Low Elastic Modulus Ti-35Nb-3Zr Alloy: Nanosurface Engineering for Enhanced Degradation Resistance. ACS Biomaterials Science and Engineering, 2017, 3, 509-517.	2.6	17
52	Phenomena of Nano- and Micro-Pore Formation on Ti-(10~50)Ta Alloys by Plasma Electrolytic Oxidation for Dental Implants. Journal of Nanoscience and Nanotechnology, 2017, 17, 2285-2290.	0.9	6
53	Electrochemical deposition behavior and characterization of Pd-Ag-HAp nanoparticles on ultra-fine TiO 2 nanotubes. Surface and Coatings Technology, 2017, 320, 383-390.	2.2	16
54	Electrochemical characteristics of Ti-6Al-4V after plasma electrolytic oxidation in solutions containing Ca, P, and Zn ions. Surface and Coatings Technology, 2017, 320, 458-466.	2.2	42

#	Article	IF	CITATIONS
55	Manganese Coatings on Hydroxyapatite-Deposited Ti–29Nb–xHf Alloys After Nanomesh Formation. Journal of Nanoscience and Nanotechnology, 2017, 17, 2661-2665.	0.9	1
56	Surface Characteristics of Nanotube Formed Ti–25Nb–xZr Alloys. Journal of Nanoscience and Nanotechnology, 2017, 17, 2655-2660.	0.9	2
57	Effects of Electrolyte Concentration on Formation of Calcium Phosphate Films on Ti–6Al–4V by Electrochemical Deposition. Journal of Nanoscience and Nanotechnology, 2017, 17, 2743-2746.	0.9	7
58	Nanosized Hydroxyapatite Precipitation on the Ti—30Ta— <i>x</i> Hf Alloys. Journal of Nanoscience and Nanotechnology, 2017, 17, 2596-2600.	0.9	0
59	Ultra-Fine HAp Nanoparticles Synthesized Onto TiO2 Barrier-Type Oxide Film for Biocompatibility. Journal of Nanoscience and Nanotechnology, 2017, 17, 3903-3908.	0.9	Ο
60	Effect of different grinding burs on the physical properties of zirconia. Journal of Advanced Prosthodontics, 2016, 8, 137.	1.1	24
61	Nano-Sized Hydroxyapatite Coating on Ti– <i>x</i> Ta Alloys for Dental Materials. Journal of Nanoscience and Nanotechnology, 2016, 16, 11022-11030.	0.9	Ο
62	Reprint of "Hydroxyapatite deposition on micropore-formed Ti-Ta-Nb alloys by plasma electrolytic oxidation for dental applications― Surface and Coatings Technology, 2016, 307, 1152-1157.	2.2	4
63	Hydroxyapatite deposition on micropore-formed Ti-Ta-Nb alloys by plasma electrolytic oxidation for dental applications. Surface and Coatings Technology, 2016, 294, 15-20.	2.2	18
64	Bone-like apatite formation on manganese-hydroxyapatite coating formed on Ti-6Al-4V alloy by plasma electrolytic oxidation. Thin Solid Films, 2016, 620, 126-131.	0.8	34
65	Hydroxyapatite-silicon film deposited on Ti–Nb–10Zr by electrochemical and magnetron sputtering method. Thin Solid Films, 2016, 620, 114-118.	0.8	12
66	Electrochemically-coated hydroxyapatite films on nanotubular Ti Nb alloys prepared in solutions containing Ca, P, and Zn ions. Thin Solid Films, 2016, 620, 132-138.	0.8	15
67	Variations of nanotubes on the Ti–Nb–Hf alloys with applied voltages. Thin Solid Films, 2016, 620, 119-125.	0.8	8
68	Surface Characteristics of Nano-Structured Silicon/Hydroxyapatite Deposition onto the Ti–Nb–Zr Alloy. Journal of Nanoscience and Nanotechnology, 2016, 16, 1783-1786.	0.9	5
69	Biocompatibility of Mg Ion Doped Hydroxyapatite Films on Ti–6Al–4V Surface by Electrochemical Deposition. Journal of Nanoscience and Nanotechnology, 2016, 16, 1405-1409.	0.9	3
70	Effect of the Mg Ion Containing Oxide Films on the Biocompatibility of Plasma Electrolytic Oxidized Ti-6Al-4V. Journal of the Korean Institute of Surface Engineering, 2016, 49, 135-140.	0.1	9
71	Fractured Surface Morphology and Mechanical Properties of Ni-Cr Based Alloys with Mo Content for Dental Applications. Journal of the Korean Institute of Surface Engineering, 2016, 49, 260-264.	0.1	0
72	Microstructure and Mechanical Properties of Rod Wire and Dental Co–Cr Alloy before and after Casting. Science of Advanced Materials, 2016, 8, 2241-2247.	0.1	0

#	Article	IF	CITATIONS
73	Corrosion Properties of Ni–13Cr–(4â^1⁄410)Mo for Dental Casting Alloys. Science of Advanced Materials, 2016, 8, 2248-2252.	0.1	Ο
74	Porcelain Bonding Strength and Mechanical Properties of Sintered Ni-Cr-Ti Alloy for Dental Prosthodontics. Journal of the Korean Institute of Surface Engineering, 2016, 49, 560-566.	0.1	0
75	Highly ordered nanotubular film formation on Ti–25Nb–xZr and Ti–25Ta–xHf. Thin Solid Films, 2015, 596, 94-100.	0.8	4
76	Electrochemical Characteristics of Cell Cultured Ti–Nb–Zr Alloys After Nano-Crystallized Si-HA Coating. Journal of Nanoscience and Nanotechnology, 2015, 15, 185-188.	0.9	2
77	Nano-Particle Formation of Mn/HA on the Ti-35Ta- <l>x</l> Nb Alloy by Electrochemical Methods. Journal of Nanoscience and Nanotechnology, 2015, 15, 6120-6123.	0.9	0
78	Nanotube Nucleation Phenomena of Titanium Dioxide on the Ti–6Al–4V Alloy Using Anodic Titanium Oxide Technique. Journal of Nanoscience and Nanotechnology, 2015, 15, 467-470.	0.9	3
79	Surface morphology of Zn-containing hydroxyapatite (Zn-HA) deposited electrochemically on Ti–xNb alloys. Thin Solid Films, 2015, 587, 163-168.	0.8	11
80	Nanotubular Structure on the Ti–29Nb–5Zr Alloy by Scanning Transmission Electron Microscope. Journal of Nanoscience and Nanotechnology, 2015, 15, 595-599.	0.9	3
81	Electrochemical Deposition of Si-Ca/P on Nanotube Formed Beta Ti Alloy by Cyclic Voltammetry Method. Journal of Nanoscience and Nanotechnology, 2015, 15, 6124-6128.	0.9	2
82	The Control of Nanotube Morphology Using Various Factors for Dental Implant. Journal of Nanoscience and Nanotechnology, 2015, 15, 181-184.	0.9	0
83	Low elastic modulus Ti–Ta alloys for load-bearing permanent implants: Enhancing the biodegradation resistance by electrochemical surface engineering. Materials Science and Engineering C, 2015, 46, 226-231.	3.8	25
84	Effects of TiN Coating on the Fatigue Fracture of Dental Implant System with Various Cyclic Loads. Journal of the Korean Institute of Surface Engineering, 2015, 48, 283-291.	0.1	0
85	AC Impedance Behaviors of Electrochemically Deposited Si–Hydroxyapatite Films on Nanotube-Formed Ti–Nb–Zr Alloys. Journal of Nanoscience and Nanotechnology, 2014, 14, 9014-9019.	0.9	2
86	Electrochemical and Sputtering Deposition of Hydroxyapatite Film on Nanotubular Ti–25Ta– <i>x</i> Zr Alloys. Journal of Nanoscience and Nanotechnology, 2014, 14, 8405-8410.	0.9	2
87	Hydroxyapatite Precipitation on Nanotube Surfaces of Ti–35Ta– <i>x</i> Nb Alloys. Journal of Nanoscience and Nanotechnology, 2014, 14, 7581-7584.	0.9	4
88	Nanotube Nucleation Phenomena on Ti–25Ta– <l>x</l> Zr Alloys for Implants Using ATO Technique. Journal of Nanoscience and Nanotechnology, 2014, 14, 7569-7573.	0.9	4
89	Hydroxyapatite formation on biomedical Ti–Ta–Zr alloys by magnetron sputtering and electrochemical deposition. Thin Solid Films, 2014, 572, 119-125.	0.8	27
90	Control of nanotube shape and morphology on Ti–Nb(Ta)–Zr alloys by varying anodizing potential. Thin Solid Films, 2014, 572, 105-112.	0.8	19

#	Article	IF	CITATIONS
91	Electrochemical behavior of hydroxyapatite/TiN multi-layer coatings on Ti alloys. Thin Solid Films, 2014, 572, 113-118.	0.8	15
92	Preparation of silicon-substituted hydroxyapatite coatings on Ti–30Nb–xTa alloys using cyclic electrochemical deposition method. Thin Solid Films, 2014, 572, 99-104.	0.8	16
93	Surface Morphology of Nanotube Formed Ti Alloy by Electrochemical Methods. Journal of Nanoscience and Nanotechnology, 2014, 14, 8372-8376.	0.9	2
94	Surface characteristics of hydroxyapatite coatings on nanotubular Ti–25Ta–xZr alloys prepared by electrochemical deposition. Surface and Coatings Technology, 2014, 259, 274-280.	2.2	13
95	Morphology change of HA films on highly ordered nanotubular Ti–Nb–Hf alloys as a function of electrochemical deposition cycle. Surface and Coatings Technology, 2014, 259, 281-289.	2.2	14
96	Effects of TiN and WC coating on the fatigue characteristics of dental implant. Surface and Coatings Technology, 2014, 243, 71-81.	2.2	21
97	Morphology of hydroxyapatite nanoparticles in coatings on nanotube-formed Ti–Nb–Zr alloys for dental implants. Vacuum, 2014, 107, 297-303.	1.6	29
98	Biocompatibility of Nanotube Formed Ti–30Nb–7Ta Alloys. Journal of Nanoscience and Nanotechnology, 2014, 14, 8427-8431.	0.9	1
99	Surface Characteristics of HA Coating and Micro-Pore Formation on the Ti–25Nb– <i>x</i> Hf Alloys for Dental Materials. Journal of Nanoscience and Nanotechnology, 2014, 14, 7745-7750.	0.9	0
100	Optimization of Nano-Etching Treatment for Bonding Strength Between Zirconia and Veneering Porcelain. Journal of Nanoelectronics and Optoelectronics, 2014, 9, 76-82.	0.1	0
101	AC impedance behavior of silicon-hydroxyapatite doped film on the Ti–35Nb–xZr alloy by EB-PVD method. Surface and Coatings Technology, 2013, 228, S505-S510.	2.2	14
102	Photofunctionalization of EB-PVD HA-coated nano-pore surface of Ti–30Nb–xZr alloy for dental implants. Surface and Coatings Technology, 2013, 228, S470-S476.	2.2	14
103	Hydroxyapatite precipitation on nanotubular films formed on Ti-6Al-4V alloy for biomedical applications. Thin Solid Films, 2013, 549, 135-140.	0.8	29
104	Surface characteristics of hydroxyapatite-coated layer prepared on nanotubular Ti–35Ta–xHf alloys by EB-PVD. Thin Solid Films, 2013, 549, 147-153.	0.8	9
105	Formation of titanium dioxide nanotubes on Ti–30Nb–xTa alloys by anodizing. Thin Solid Films, 2013, 549, 141-146.	0.8	27
106	Hydroxyapatite coating on micropore-formed titanium alloy utilizing electrochemical deposition. Thin Solid Films, 2013, 549, 154-158.	0.8	23
107	Hydroxyapatite thin film coatings on nanotube-formed Ti–35Nb–10Zr alloys after femtosecond laser texturing. Surface and Coatings Technology, 2013, 217, 13-22.	2.2	35
108	Bioactivity evaluation of porous TiO2 surface formed on titanium in mixed electrolyte by spark anodization. Surface and Coatings Technology, 2013, 235, 706-713.	2.2	33

#	Article	IF	CITATIONS
109	Surface characteristics of hydroxyapatite films deposited on anodized titanium by an electrochemical method. Thin Solid Films, 2013, 546, 185-188.	0.8	21
110	Surface morphology of TiN-coated nanotubular Ti–25Ta–xZr alloys for dental implants prepared by RF sputtering. Thin Solid Films, 2013, 549, 131-134.	0.8	11
111	Plasma deposition of a silicone-like layer for the corrosion protection of magnesium. Progress in Organic Coatings, 2013, 76, 1827-1832.	1.9	15
112	Silicon-substituted hydroxyapatite coating with Si content on the nanotube-formed Ti–Nb–Zr alloy using electron beam-physical vapor deposition. Thin Solid Films, 2013, 546, 189-195.	0.8	18
113	Surface Morphology of Highly Ordered Nanotube Formed and Laser Textured Beta Titanium Alloys. Journal of Nanoscience and Nanotechnology, 2013, 13, 1876-1879.	0.9	3
114	Electrochemical Characteristics of TiN/ZrN Multilayers on the Ti–35Ta–xHf Alloy by Magnetron Sputtering. Japanese Journal of Applied Physics, 2013, 52, 11NB06.	0.8	0
115	Surface Observation of Nanotube/Micropit Formed Ti–Nb– <i>x</i> Zr Alloy for Biocompatibility. Journal of Nanoscience and Nanotechnology, 2013, 13, 1706-1709.	0.9	1
116	Surface Phenomena of Hydroxyapatite Film on the Nanopore Formed Ti–29Nb– <i>x</i> Zr Alloy by Anodization for Bioimplants. Journal of Nanoscience and Nanotechnology, 2013, 13, 1679-1683.	0.9	4
117	Effect of various intraoral repair systems on the shear bond strength of composite resin to zirconia. Journal of Advanced Prosthodontics, 2013, 5, 248.	1.1	33
118	Effect of coating on properties of esthetic orthodontic nickel-titanium wires. Angle Orthodontist, 2012, 82, 319-325.	1.1	62
119	Formation of Nano-Phase Hydroxyapatite Film on TiO ₂ Nano-Network. Journal of Nanoscience and Nanotechnology, 2012, 12, 822-827.	0.9	9
120	Electrochemical and surface behavior of hydyroxyapatite/Ti film on nanotubular Ti–35Nb–xZr alloys. Applied Surface Science, 2012, 258, 2129-2136.	3.1	29
121	Surface characteristics of TiN/ZrN coated nanotubular structure on the Ti–35Ta–xHf alloy for bio-implant applications. Applied Surface Science, 2012, 258, 2088-2092.	3.1	16
122	Surface phenomena of HA/TiN coatings on the nanotubular-structured beta Ti–29Nb–5Zr alloy for biomaterials. Applied Surface Science, 2012, 258, 2083-2087.	3.1	14
123	Effects of TiN coating on the corrosion of nanostructured Ti–30Ta–xZr alloys for dental implants. Applied Surface Science, 2012, 258, 1929-1934.	3.1	39
124	Comparison of fatigue fracture strength by fixture diameter of mini implants. The Journal of Korean Academy of Prosthodontics, 2012, 50, 156.	0.0	1
125	Enhanced research of nanotubularâ€structured Tiâ€35Nbâ€xZr alloys for biomaterials using STEM. Surface and Interface Analysis, 2012, 44, 1462-1467.	0.8	3
126	Measurement of oxide thin film dissolution rate on the HA-coated Ti alloy by scanning electron microscopy and impedance spectroscopy. Surface and Interface Analysis, 2012, 44, 1468-1472.	0.8	6

#	Article	IF	CITATIONS
127	Nanotube growth analysis in the interface between oxide film and titanium alloy substrate using STEM and FEâ€SEM. Surface and Interface Analysis, 2012, 44, 1473-1478.	0.8	4
128	Transmission electron microscopy application for the phenomena of hydroxyapatite precipitation in microporeâ€structured Ti alloy. Surface and Interface Analysis, 2012, 44, 1492-1496.	0.8	3
129	Effects of Hafnium Addition on the Pitting Corrosion Behavior of Ti Alloys in Electrolyte Containing Chloride Ion. Corrosion Science and Technology, 2012, 11, 191-195.	0.2	о
130	Electrochemical Oxide Nanotube Formation on the Ti-35Ta-xHf Alloys for Dental Materials. Journal of Nanoscience and Nanotechnology, 2011, 11, 7428-7432.	0.9	4
131	Nanotubular Oxide Surface and Layer Formed on the Ti-35Ta-xZr Alloys for Biomaterials. Journal of Nanoscience and Nanotechnology, 2011, 11, 7433-7437.	0.9	5
132	Corrosion Behavior of Nanotubular Oxide on the Ti–29Nb–xZr Alloy. Journal of Nanoscience and Nanotechnology, 2011, 11, 1636-1639.	0.9	3
133	Morphology of hydroxyapatite coated nanotube surface of Ti–35Nb–xHf alloys for implant materials. Thin Solid Films, 2011, 520, 793-799.	0.8	26
134	Corrosion characteristics of anodized Ti–(10–40wt%)Hf alloys for metallic biomaterials use. Journal of Materials Science: Materials in Medicine, 2011, 22, 41-50.	1.7	24
135	Fatigue Fracture of Implant System Using TiN and WC Coated Abutment Screw. Procedia Engineering, 2011, 10, 680-685.	1.2	8
136	Microscopic Analysis of Fractured Dental Implant Surface after Clinical UseR. Procedia Engineering, 2011, 10, 1955-1960.	1.2	12
137	Evaluation of Interfacial Bonding Strength between Laser Textured Metal Coping and Porcelain. Procedia Engineering, 2011, 10, 2286-2291.	1.2	9
138	Formation of Surface Roughness on the Ti-35Nb-xZr Alloy Using Femtosecond Laser for Biocompatibility. Procedia Engineering, 2011, 10, 2393-2398.	1.2	15
139	Nanotubular surface and morphology of Ti-binary and Ti-ternary alloys for biocompatibility. Thin Solid Films, 2011, 519, 4652-4657.	0.8	45
140	Nanostructured surface changes of Ti–35Ta–xZr alloys with changes in anodization factors. Thin Solid Films, 2011, 519, 4663-4667.	0.8	8
141	Nanostructured thin film formation on femtosecond laser-textured Ti–35Nb–xZr alloy for biomedical applications. Thin Solid Films, 2011, 519, 4668-4675.	0.8	29
142	Hydroxyapatite coating on the Ti–35Nb–xZr alloy by electron beam-physical vapor deposition. Thin Solid Films, 2011, 519, 7050-7056.	0.8	36
143	Surface characteristics of hydroxyapatite/titanium composite layer on the Ti-35Ta-xZr surface by RF and DC sputtering. Thin Solid Films, 2011, 519, 7045-7049.	0.8	26
144	Electrochemical Behavior of Nano and Femtosecond Laser Textured Titanium Alloy for Implant Surface Modification. Journal of Nanoscience and Nanotechnology, 2011, 11, 1581-1584.	0.9	20

#	Article	IF	CITATIONS
145	Nanotube Morphology and Corrosion Resistance of a Low Rigidity Quaternary Titanium Alloy for Biomedical Applications. Journal of Nanoscience and Nanotechnology, 2010, 10, 4635-4639.	0.9	1
146	The biocompatibility of HA thin films deposition on anodized titanium alloys. Surface and Coatings Technology, 2010, 205, S267-S270.	2.2	35
147	Surface characteristics of HA coated Ti-30Ta-xZr and Ti-30Nb-xZr alloys after nanotube formation. Surface and Coatings Technology, 2010, 205, S305-S311.	2.2	47
148	Phenomena of Nanotube Nucleation and Growth on New Ternary Titanium Alloys. Journal of Nanoscience and Nanotechnology, 2010, 10, 4684-4689.	0.9	18
149	Corrosion Behavior of Nanotube Formed on the Bone Plate of Ti-6Al-4V Alloy for Dental Use. Journal of the Korean Institute of Surface Engineering, 2010, 43, 25-30.	0.1	0
150	Surface Characteristics of Dental Implant Fixture with Various Manufacturing Process. Journal of the Korean Institute of Surface Engineering, 2010, 43, 17-24.	0.1	0
151	Surface Characteristics of Polymer Coated NiTi Alloy Wire for Orthodontics. Journal of the Korean Institute of Surface Engineering, 2010, 43, 132-141.	0.1	0
152	Surface Characteristics of TiN and ZrN Film Coated STD 61 by Sputtering. Journal of the Korean Institute of Surface Engineering, 2010, 43, 260-265.	0.1	0
153	An electrochemical study on self-ordered nanoporous and nanotubular oxide on Ti–35Nb–5Ta–7Zr alloy for biomedical applications. Acta Biomaterialia, 2009, 5, 2303-2310.	4.1	107
154	Nanotube morphology changes for Ti–Zr alloys as Zr content increases. Thin Solid Films, 2009, 517, 5033-5037.	0.8	64
155	Electrochemical characteristics of nanotubes formed on Ti–Nb alloys. Thin Solid Films, 2009, 517, 5038-5043.	0.8	84
156	Nanotube formation and morphology change of Ti alloys containing Hf for dental materials use. Thin Solid Films, 2009, 517, 5365-5369.	0.8	27
157	Electrochemical behavior of Co-Cr and Ni-Cr dental cast alloys. Transactions of Nonferrous Metals Society of China, 2009, 19, 785-790.	1.7	52
158	Electrochemical behavior of dental implant system before and after clinical use. Transactions of Nonferrous Metals Society of China, 2009, 19, 846-851.	1.7	6
159	Surface characteristics of HA coated Ti-Hf binary alloys after nanotube formation. Transactions of Nonferrous Metals Society of China, 2009, 19, 852-856.	1.7	22
160	Effects of TiN film coating on electrochemical behaviors of nanotube formed Ti-xHf alloys. Transactions of Nonferrous Metals Society of China, 2009, 19, 857-861.	1.7	9
161	Mechanical properties and corrosion resistance of low rigidity quaternary titanium alloy for biomedical applications. Transactions of Nonferrous Metals Society of China, 2009, 19, 862-865.	1.7	17
162	Nanostructure and corrosion behaviors of nanotube formed Ti-Zr alloy. Transactions of Nonferrous Metals Society of China, 2009, 19, 1005-1008.	1.7	51

#	Article	IF	CITATIONS
163	Electrochemical Behaviors of a TiN-Coated/Nanotube-formed Ti-Zr Alloy. Journal of the Korean Physical Society, 2009, 54, 1036-1041.	0.3	5
164	Electrochemical Properties of Ti-30Ta-(3~15)Nb Alloys Coated by HA/Ti Compound Layer. Journal of the Korean Institute of Surface Engineering, 2008, 41, 57-62.	0.1	1
165	Interface activation and surface characteristics of Ti/TiN/HA coated sintered stainless steels. Metals and Materials International, 2006, 12, 31-37.	1.8	6
166	Degradation phenomena of magnetic attachments used clinically in the oral environment. Metals and Materials International, 2006, 12, 357-364.	1.8	2
167	Electrochemical behavior of TiN film coated Tiâ^ Nb alloys for dental materials. Metals and Materials International, 2006, 12, 365-369.	1.8	13
168	Surface characteristics of clinically used dental implant screws. Metals and Materials International, 2005, 11, 449-456.	1.8	8
169	Corrosion behavior between dental implant abutment and cast gold alloy. Metals and Materials International, 2004, 10, 153-159.	1.8	8
170	Effect of surface coating on the screw loosening of dental abutment screws. Metals and Materials International, 2004, 10, 549-553.	1.8	9
171	Analyses of fractured implant fixture after prolonged implantation. Metals and Materials International, 2004, 10, 327-335.	1.8	16
172	Correlation of immunohistochemical characteristics of the craniomandibular joint with the degree of mandibular lengthening in rabbits. Journal of Oral and Maxillofacial Surgery, 2003, 61, 1189-1197.	0.5	11
173	Effects of nitrogen ion implantation on the surface characteristics of iron aluminides. Surface and Coatings Technology, 2001, 148, 77-86.	2.2	8
174	Corrosion Characteristics of EB-PVD Ti/TiN Multi-layer Film Coated Sm-Co and Fe-Nd-B Magnets. Nippon Kinzoku Gakkaishi/Journal of the Japan Institute of Metals, 2001, 65, 253-261.	0.2	2
175	Effects of nitrogen ion implantation on the corrosion characteristics of Cu-electroless plated and sintered stainless steel. Surface and Coatings Technology, 1999, 112, 299-306.	2.2	13
176	Effects of Cr, Mo and B on the Corrosion Behavior of Fe3Al Intermetallic Compounds. Zairyo To Kankyo/ Corrosion Engineering, 1996, 45, 122-130.	0.0	4
177	Stress Corrosion Behavior of Ni-Ti Shape Memory Alloys in High Temperature Water. Nippon Kinzoku Gakkaishi/Journal of the Japan Institute of Metals, 1996, 60, 577-581.	0.2	2
178	Antibacterial activity and surface characteristics of nanotube-formed Ti–xNb–Ag–Pt alloy. Applied Nanoscience (Switzerland), 0, , .	1.6	0